Regional high-resolution spatiotemporal gravity modeling from GRACE data using spherical wavelets

M. Schmidt,[1] S.-C. Han,[2] J. Kusche,[3] L. Sanchez,[1] and C. K. Shum[2]

Received 16 December 2005; revised 13 February 2006; accepted 2 March 2006; published 26 April 2006.

[1] We determine a regional spatiotemporal gravity field over northern South America including the Amazon region using GRACE inter-satellite range-rate measurements by application of a wavelet-based multiresolution technique. A major advantage of this method is that we are able to represent the Amazon hydrological signals in form of time series of detail signals with level-dependent temporal resolution: the coarser structures generally require only ten days, whereas the medium and finer details are computable from one month of data. To this end, we employ the basic property of multiresolution representations, which is to split a signal into detail signals, each related to a specific resolution level and computable from data covering a specific part of the spectrum. Our results, which for the first time fully exploit the spatial and temporal resolutions of GRACE data in modeling Amazon hydrological fluxes, are in good agreement with hydrological models and GPS-derived height variations. **Citation:** Schmidt, M., S.-C. Han, J. Kusche, L. Sanchez, and C. K. Shum (2006), Regional high-resolution spatiotemporal gravity modeling from GRACE data using spherical wavelets, *Geophys. Res. Lett.*, *33*, L08403, doi:10.1029/2005GL025509.

1. Introduction

[2] Traditionally in satellite gravity recovery problems the global gravity field of the Earth has been modeled as a spherical harmonic expansion [*Tapley et al.*, 2004a; *Reigber et al.*, 2005]. Recently available low-low satellite-to-satellite tracking data from the Gravity and Climate Experiment (GRACE) mission have been used to derive time-variable gravity fields for fixed time intervals, like one month, independently on the frequency structure [*Tapley et al.*, 2004b]. Limitations with this approach include:

[3] 1. Whereas it is possible to estimate the low degree harmonics from only a few weeks of GRACE data, the high degree harmonics are weakly determined and highly contaminated by noise.

[4] 2. The estimation procedure, e.g., the choice of the truncation degree of the spherical harmonic expansion, can neither be adapted to the regional variability of the gravity signal due to the specific hydrological setting or due to other geophysical processes nor be conformed to the increase of spatial resolution as the satellites move closer to the polar regions.

[5] For these reasons, low-pass filters are typically applied in the final interpretation of GRACE spherical harmonic coefficients [*Swenson and Wahr*, 2002]. It appears reasonable to replace this two-step procedure by a more direct approach. Recent GRACE studies have represented the sources of gravity field changes directly in terms of discretizing a surface mass layer [*Rowlands et al.*, 2005; *Han et al.*, 2005]; this allows to regionally tune the estimation by incorporating constraints, but it does not yet allow level-dependent temporal resolution, as it does not provide a multiresolution representation (MRR).

[6] In this paper, we apply quasi-compactly supported spherical scaling functions and wavelets to construct spatiotemporal gravity fields as MRRs [*Freeden et al.*, 1998; *Schmidt et al.*, 2005] from GRACE data sets, geographically given in northern South America including the Amazon basin and temporarily restricted to (resolution) level-dependent, i.e., frequency-dependent time intervals of ten days and one month. The results are then validated with independent models and data.

2. Multiresolution Representation

[7] The MRR of the Earth's geopotential $V(\boldsymbol{x}, t)$, thought as a general input signal depending on position vector $\boldsymbol{x} = |\boldsymbol{x}|\ \boldsymbol{r}$ and time t, can be written as

$$V(\boldsymbol{x},t) = \overline{V}(\boldsymbol{x},t) + \sum_{i=i'}^{I} v_i(\boldsymbol{x},t) + s(\boldsymbol{x},t) \tag{1}$$

[*Schmidt et al.*, 2005]. Herein, $\overline{V}(\boldsymbol{x},t)$ means a reference model, e.g., a spherical harmonic expansion up to a certain degree, possibly including time-variable coefficients; $s(\boldsymbol{x},t)$ absorbs all unmodeled signal parts. In our approach a detail signal $v_i(\boldsymbol{x},t)$ of resolution level (scale) i is defined as the spherical convolution

$$v_i(\boldsymbol{x},t) = [\psi_i \star \delta V(\cdot,t)](\boldsymbol{x}) \tag{2}$$

of the residual geopotential $\delta V(\boldsymbol{x}_R,t) := V(\boldsymbol{x}_R,t) - \overline{V}(\boldsymbol{x}_R,t)$ given on a sphere Ω_R (R = radius), i.e., $\boldsymbol{x}_R = |\boldsymbol{x}_R|\boldsymbol{r}_R \in \Omega_R$, with the spherical wavelet ψ_i. Since its Legendre series expansion $\psi_i(\boldsymbol{x},\boldsymbol{x}_R) = \sum_n \frac{2n+1}{4\pi R^2}\left(\frac{R}{|\boldsymbol{x}|}\right)^{n+1}\Psi_{i,n}P_n(\boldsymbol{r}^T\boldsymbol{r}_R)$ includes the harmonical continuation into the outer space $\underline{\Omega_R^{\text{ext}}}$ of Ω_R, the detail signal $v_i(\boldsymbol{x},t)$ is computable for all $\boldsymbol{x} \in \Omega_R^{\text{ext}} = \Omega_R^{\text{ext}} \cup \Omega_R$; the functions $P_n(\boldsymbol{r}^T\boldsymbol{r}_R)$ are the Legendre polynomials of degree n depending on the spherical distance $\alpha = \arccos(\boldsymbol{r}^T\boldsymbol{r}_R)$. The MRR as defined by the equations (1) and (2) is based on a two-scale relation. In linear wavelet theory

[1]Deutsches Geodätisches Forschungsinstitut, Munich, Germany.
[2]Laboratory for Space Geodesy and Remote Sensing Research, Ohio State University, Columbus, Ohio, USA.
[3]Department of Earth Observation and Space Systems, Delft University of Technology, Delft, Netherlands.

0094-8276/06/2005GL025509

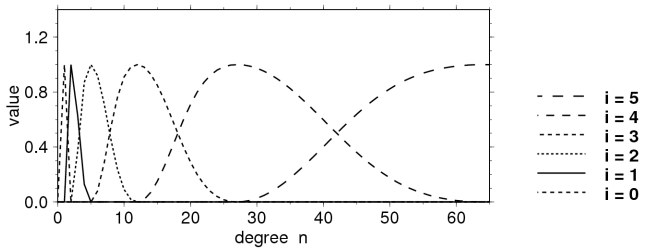

Figure 1. Legendre coefficients $\Psi_{i,n}$ of Blackman wavelets ψ_i for levels $i = 0, \ldots, 5$; compare also Schmidt et al. (submitted manuscript, 2005).

this two-scale relation reads $\psi_i = \phi_{i+1} - \phi_i$ and defines the spherical wavelet ψ_i as the difference of the spherical scaling functions ϕ_{i+1} and ϕ_i of the consecutive levels $i + 1$ and i (M. Schmidt et al., Regional gravity modelling in terms of spherical base functions, submitted to *Journal of Geodesy*, 2005, hereinafter referred to as Schmidt et al., submitted manuscript, 2005). Since a scaling function can be identified with a low-pass filter, a wavelet acts as a band-pass filter. Among a large number of appropriate spherical scaling functions we chose the Blackman function (Schmidt et al., submitted manuscript, 2005), because the corresponding Blackman wavelet is quasi-compact on the sphere and strictly band-limited in the frequency domain as illustrated in Figure 1; the shown Legendre coefficients $\Psi_{i,n}$ reflect the frequency behavior. The higher the level value i is chosen the finer are the structures extractable from the input data according to equation (2). This localizing feature is one of the most important arguments why spherical wavelets are more advantageous in enhancing signal resolutions for regional modeling than spherical harmonics.

[8] For numerical computations we replace the spherical convolution in favor of the series expansion

$$v_i(\boldsymbol{x},t) = \sum_{k=1}^{N_i} d_{i,k}(t)\ \psi_i(\boldsymbol{x},\boldsymbol{x}_{i,k}) \tag{3}$$

in terms of spherical wavelet (base) functions $\psi_i(\boldsymbol{x},\boldsymbol{x}_{i,k})$, related to N_i level$-i$ computation points with position vectors $\boldsymbol{x}_{i,k} \in \Omega_R$. The time-dependent scaling coefficients $d_{i,k}(t)$ are the solve-for parameters in this formulation of the satellite gravity recovery problem.

[9] Considering the above mentioned two-scale relation in equation (2) we obtain from equation (1) $\delta V(\boldsymbol{x},t) = V(\boldsymbol{x},t) - \overline{V}(\boldsymbol{x},t) = \sum_{i=i'}^{I}[\psi_i \star \delta V(\cdot,t)](\boldsymbol{x}) + s(\boldsymbol{x},t) = [\phi_{I+1} \star \delta V(\cdot,t)](\boldsymbol{x}) + s(\boldsymbol{x},t)$. Since the spherical convolution $\phi_{I+1} \star \delta V$ can be rewritten as series expansion in terms of spherical scaling (base) functions $\phi_{I+1}(\boldsymbol{x},\boldsymbol{x}_{I,k})$ related to N_I level$-I$ computation points with position vectors $\boldsymbol{x}_{I,k} \in \Omega_R$, the representation

$$\delta V(\boldsymbol{x},t) = \sum_{k=1}^{N_I} d_{I,k}(t)\ \phi_{I+1}(\boldsymbol{x},\boldsymbol{x}_{I,k}) + s(\boldsymbol{x},t) \tag{4}$$

follows. After determining the scaling coefficients $d_{I,k}(t)$ they can be used to compute the detail signal $v_I(\boldsymbol{x},t)$ according to equation (3) for $i = I$ and to start the pyramid algorithm for calculating the scaling coefficients $d_{i,k}(t)$ as well as the detail signals $v_i(\boldsymbol{x},t)$ of the lower levels $i = i', \ldots, I-1$ (Schmidt et al., submitted manuscript, 2005). However, from equation (2) together with Figure 1 we expect that different detail signals $v_i(\boldsymbol{x},t)$ would be more sensitive to particular input signals $\delta V(\boldsymbol{x},t) =: \delta V_i(\boldsymbol{x},t)$ in dependence on their spectral behavior and noise characteristics. As described in the following our procedure to construct a spatiotemporal gravity field is based on this expectation.

3. Spatiotemporal Gravity Field

3.1. GRACE Input Data

[10] We processed the GRACE L1B data, i.e., KBR and accelerometer data as well as precise orbits from University of Texas (S. Bettadpur, personal communication, 2005), via the energy balance approach into residual GRACE geopotential difference observations $\Delta V_{1,2}(t) = \delta V(\boldsymbol{x}_1,t) - \delta V(\boldsymbol{x}_2,t)$ [*Jekeli*, 1999; *Han et al.*, 2006]. The terms $\delta V(\boldsymbol{x}_l,t)$ with $l \in \{1,2\}$ are the residual GRACE geopotential values $\delta V(\boldsymbol{x}_l,t) = V(\boldsymbol{x}_l,t) - \overline{V}(\boldsymbol{x}_l)$, here defined as the difference between the geopotential $V(\boldsymbol{x}_l,t)$ and the static reference model $\overline{V}(\boldsymbol{x}_l)$ along the trajectories $\boldsymbol{x}_1 = \boldsymbol{x}_1(t)$ and $\boldsymbol{x}_2 = \boldsymbol{x}_2(t)$ of the two GRACE satellites. For $\overline{V}(\boldsymbol{x}_l)$ we chose GGM01C [*Tapley et al.*, 2004a]. Geographically we used only data from a rectangular region in northern South America including the Amazon basin (see Figure 2) within an observation interval between February 2003 and December 2003 (except June) with a sampling rate of five seconds. The observations are corrected by a priori time-variable gravitational potentials w.r.t. planetary bodies, tides, oceans and atmosphere; for details, see *Han et al.* [2005]. Hence, the remaining residual GRACE geopotential difference observations $\Delta V_{1,2}(t) =: \Delta V_{1,2}^{\mathrm{hyd}}(t)$, given at discrete times $t = t_j$ with an a priori standard deviation of approximately 0.003 $\mathrm{m}^2/\mathrm{s}^2$, primarily reflect the hydrology variations over the continent.

[11] Based on this scenario we created various GRACE data sets by dividing the total observation interval $\Delta T =$ [1 January, 31 December] into M_i level-dependent observation sub-intervals ΔT_i with $\Delta T = M_i\, \Delta T_i$. Information about the corresponding level-dependent partitioning of the complete data set into sub-data sets S_{i,m_i} with $m_i = 1, \ldots, M_i$ is listed in Table 1 for levels $i = 2, 3, 4$. Our motivation for this partitioning scheme is that the determination of finer structures of the gravity field requires a denser distribution of satellite tracks than the computation of coarser structures. The observation equation for an observation $\Delta V_{1,2}^{\mathrm{hyd}}(t_j)$ of a level$-i$ data set S_{i,m_i}, i.e., $t_j \in [t_{i,m_i}, t_{i,m_i+1})$ with $t_{i,m_i+1} = t_{i,m_i} + \Delta T_i$, follows from equation (4) setting $I =: i$, defining $d_{i,k}(t_j) =: d_{i,k,m_i}$ and considering the measurement error $e(t_j)$ as

$$\Delta V_{1,2}^{\mathrm{hyd}}(t_j) + e(t_j) = \sum_{k=1}^{N_i} d_{i,k,m_i}\ \Delta\phi_{i+1}(\boldsymbol{x}_1, \boldsymbol{x}_2, \boldsymbol{x}_{i,k}) \tag{5}$$

with the three-point scaling function $\Delta\phi_{i+1}(\boldsymbol{x}_1,\boldsymbol{x}_2,\boldsymbol{x}_{i,k}) := \phi_{i+1}(\boldsymbol{x}_1(t_j),\boldsymbol{x}_{i,k}) - \phi_{i+1}(\boldsymbol{x}_2(t_j),\boldsymbol{x}_{i,k})$ neglecting the difference $s(\boldsymbol{x}_1,t_j) - s(\boldsymbol{x}_2,t_j)$. We recognize from Figure 1 that the Blackman wavelets of levels $i = 0$ and $i = 1$ extract the low-frequency part of the gravity field until degree at most $n = 4$. Consequently, we do not solve for the level-0 and level-1 detail signals from our regional data sets.

3.2. Parameter Estimation

[12] According to equation (5) the observations $\Delta V_{1,2}^{\mathrm{hyd}}(t_j)$ of each level$-i$ data set S_{i,m_i} establish a linear equation

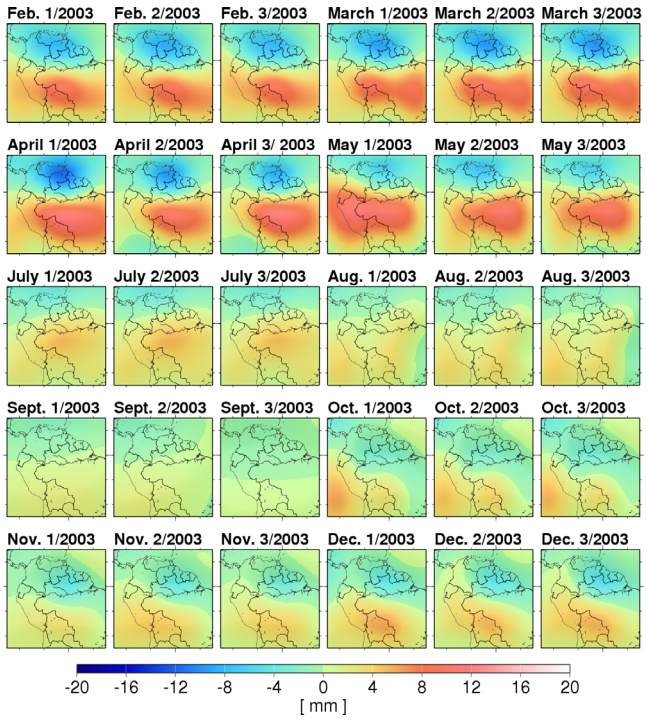

Figure 2. 10–day solutions for geoid height variations $\Delta N^{\mathrm{hyd}}(\boldsymbol{x},t)$ w.r.t. GGM01C.

system with unknown scaling coefficients d_{i,k,m_i}. Due to the downward continuation to the Earth's surface the resulting normal equation matrix is ill-conditioned. In addition, for band-limited base functions, like the Blackman scaling function, it is not even of full rank. For regularization we used a fast Monte-Carlo implementation of the iterative maximum-likelihood variance component estimation [*Koch and Kusche*, 2001]. Besides the estimators of the unknowns the covariance matrices of all quantities presented in the following are calculable applying the law of error propagation. But since these errors are probably not representative, other error estimates, e.g., based on annual fits, may be more reliable [*Tapley et al.*, 2004b].

3.3. Geoid Heights

[13] According to equation (3) the coefficients d_{i,k,m_i}, estimated from the observations $\Delta V_{1,2}^{\mathrm{hyd}}(t)$ of the data set S_{i,m_i}, provide the level–i detail signal $v_i(\boldsymbol{x},t) =: v_i^{\mathrm{hyd}}(\boldsymbol{x},t)$ with $t \in [t_{i,m_i}, t_{i,m_i+1})$. Figure 2 shows the sum of the level–2 and level–3 detail signals transformed into geoid height variations $\Delta N^{\mathrm{hyd}}(\boldsymbol{x},t) = n_2^{\mathrm{hyd}}(\boldsymbol{x},t) + n_3^{\mathrm{hyd}}(\boldsymbol{x},t)$ with $t \in [t_{2,m_2}, t_{2,m_2+1}) \subset [t_{3,m_3}, t_{3,m_3+1})$ and $\boldsymbol{x} \in \Omega_R$. Since the transformed detail signals $n_2^{\mathrm{hyd}}(\boldsymbol{x},t)$ and $n_3^{\mathrm{hyd}}(\boldsymbol{x},t)$ are 10–day and monthly solutions, respectively, the sum $\Delta N^{\mathrm{hyd}}(\boldsymbol{x},t)$ means a 10–day solution, too. According to Table 1 the altogether $M_2 = 30$ 10–day solutions consider signal parts until degree $n = 27$. Seasonal geoid height variations of about 15 mm w.r.t. the reference model GGM01C are clearly detectable.

Table 1. Level-dependent observation subinterval ΔT_i, total number M_i of level–i data sets S_{i,m_i} within the year 2003, total number p_i of observations within ΔT_i and highest degree value $n_{i,\max}$ of the level-i Blackman wavelet ψ_i according to Figure 1

Level i	Interval ΔT_i	Number of Sets M_i	Number of Observations p_i	Maximum Degree $n_{i,\max}$
2	10 days	36	4000–5000	12
3	1 month	12	13000–15000	27
4	3 months	4	20000–25000	64

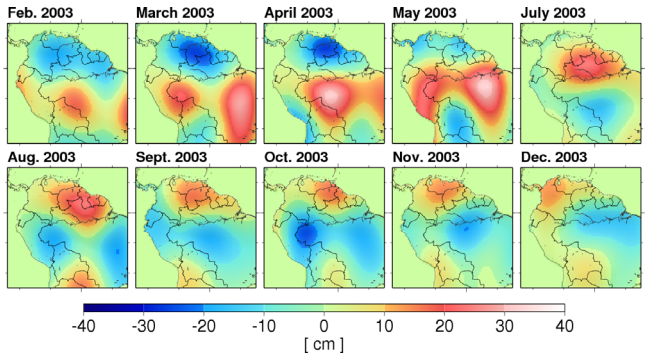

Figure 3. Monthly solutions of equivalent water heights $\Delta h^{\mathrm{ewh}}(\boldsymbol{x},t)$ over the continent from GRACE w.r.t. the mean.

3.4. Equivalent Water Heights

[14] Following Farrell's theory [*Farrell*, 1972] the estimated level–i detail signal $v_i^{\mathrm{hyd}}(\boldsymbol{x},t)$ with $\boldsymbol{x} \in \Omega_R$ can be transformed into the corresponding detail signal $h_i^{\mathrm{ewh}}(\boldsymbol{x},t)$ of so-called equivalent water heights (EWH) via the spherical convolution $h_i^{\mathrm{ewh}}(\boldsymbol{x},t) = [k^{\mathrm{ewh}} \star v_i^{\mathrm{hyd}}(\cdot,t)](\boldsymbol{x})$ with the kernel $k^{\mathrm{ewh}}(\boldsymbol{x},\boldsymbol{x}_R) = \sum_n \frac{2n+1}{4\pi R^2} \frac{(2n+1)\rho_e}{3\rho_w g\left(1+k_n'\right)} P_n(\boldsymbol{r}^T\boldsymbol{r}_R)$; ρ_e = average density of the Earth, ρ_w = density of water, g = gravitational constant and k_n' = static gravitational load Love number of degree n. Figure 3 reveals that the sum $\Delta h^{\mathrm{ewh}}(\boldsymbol{x},t) = h_2^{\mathrm{ewh}}(\boldsymbol{x},t) + h_3^{\mathrm{ewh}}(\boldsymbol{x},t)$ varies in the Amazon basin of about ±40 cm. These results are in good agreement with other investigations, e.g., with [*Han et al.*, 2005].

[15] In order to verify our results, we additionally performed a MRR of the hydrological Land Dynamics (LaD) model [*Milly and Shmakin*, 2002]. Figure 4 displays the results for the EWHs $\Delta h^{\mathrm{lad}}(\boldsymbol{x},t) = h_2^{\mathrm{lad}}(\boldsymbol{x},t) + h_3^{\mathrm{lad}}(\boldsymbol{x},t)$ of the LaD wavelet representation. Since the GRACE solutions show obviously more and up to 50% larger variations, we conclude that apart from remaining errors within the GRACE observations, the LaD model underestimates the water storage changes within the area under consideration. We obtained similar results from comparisons with other hydrology models (not shown here).

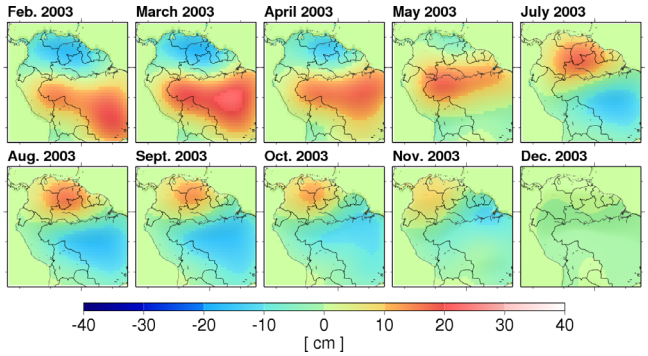

Figure 4. Monthly solutions of equivalent water heights $\Delta h^{\mathrm{lad}}(\boldsymbol{x},t)$ over the continent from the LaD model w.r.t. the mean.

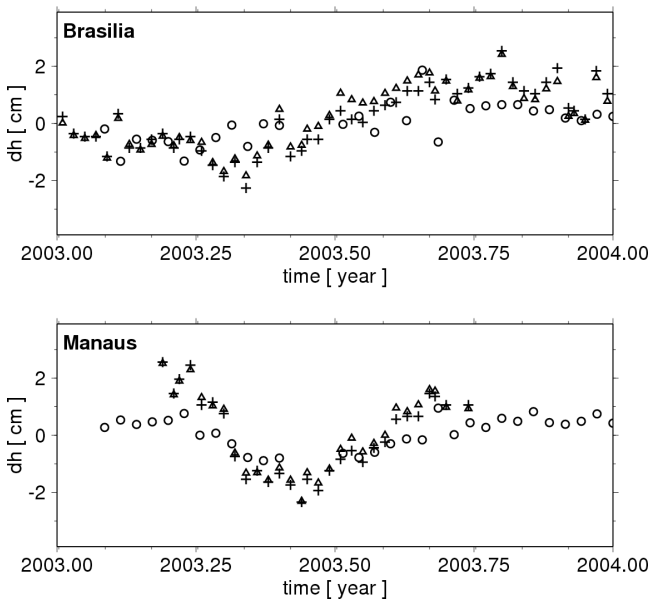

Figure 5. Time series of GPS measured height variations $\Delta h^{\mathrm{gps}}(\boldsymbol{x},t)$ (crosses); GPS height variations corrected for atmospheric loading (triangles); height deformations $\Delta h^{\mathrm{hd}}(\boldsymbol{x},t)$ derived from GRACE data (circles); all data sets w.r.t. the mean.

3.5. Height Deformations

[16] Finally we computed the detail signals $h_i^{\mathrm{hd}}(\boldsymbol{x},t)$ of height deformations (HD) at the Earth's surface by evaluating the spherical convolution $h_i^{\mathrm{hd}}(\boldsymbol{x},t) = [k^{\mathrm{hd}} \star v_i^{\mathrm{hyd}}(\cdot,t)](\boldsymbol{x})$ with the kernel $k^{\mathrm{hd}}(\boldsymbol{x},\boldsymbol{x}_R) = \sum_n \frac{2n+1}{4\pi R^2} \frac{h'_n}{g\left(1+k'_n\right)} P_n(\boldsymbol{r}^T \boldsymbol{r}_R)$; h'_n = vertical load Love number of degree n. The HDs $\Delta h^{\mathrm{hd}}(\boldsymbol{x},t) = h_2^{\mathrm{hd}}(\boldsymbol{x},t) + h_3^{\mathrm{hd}}(\boldsymbol{x},t)$ over the continent computed from 10-day solutions feature a seasonal variation of ±3 cm (not shown here). For validation we studied GPS-derived height variations $\Delta h^{\mathrm{gps}}(\boldsymbol{x},t)$ measured at the IGS stations Brasilia and Manaus in 2003 (crosses in Figure 5). Before comparing these time series with our corresponding results from GRACE, we correct $\Delta h^{\mathrm{gps}}(\boldsymbol{x},t)$ for atmospheric loading by applying the NCEP reanalysis model [*Kalnay et al.*, 1996]. Although the reduced GPS time series (triangles in Figure 5) reveal a sufficient agreement with our time series of the GRACE HDs $\Delta h^{\mathrm{hd}}(\boldsymbol{x},t)$ (circles), there are obviously deviations which might be caused by errors within the GPS time series, the atmospheric model, the loading model or due to neglecting the GRACE detail signals of levels $i = 0$ (corresponds mainly to the signal part of degree $n = 1$; see Figure 1), $i = 1$ (includes a signal part of degree $n = 2$) and $i \geq 4$ (comprise all signal parts with degree $n > 27$). The consideration of a degree $n = 1$ term in height deformations derived from GRACE data is discussed by [*Davis et al.*, 2004].

4. Conclusions

[17] We applied a regional multiresolution technique based on wavelet theory to in-situ GRACE data, computed following the energy balance approach. Various detail signals were estimated from observations spanning different periods for the corresponding levels. We calculated hydrology signals over the Amazon basin from combinations of level-2 (from degree 3 up to degree 12) and level-3 (from degree 6 up to degree 27) detail signals with temporal resolutions of ten days to one month. The presented results show a promising agreement with the LaD hydrology model and selected GPS time series of observed height variations. The MRR/wavelet approach represents a new efficient way to model spatiotemporal gravity fields with flexible temporal and spatial resolutions while fully exploit the signals of the GRACE data.

[18] **Acknowledgments.** This work is partially supported by NASA grants (NNG04GF01G and NNG04GN19G), by a grant from NGA's NURI program, and by NSF's CMG Program (EAR0327633). We acknowledge the NASA/GFZ GRACE project for the GRACE data products (distributed by JPL PODAAC), and thank Srinivas Bettadpur of the University of Texas for providing precise GRACE orbits with finer temporal resolutions for our data processing.

References

Davis, J. L., P. Elósegui, J. X. Mitrovica, and M. E. Tamisiea (2004), Climate-driven deformation of the solid Earth from GRACE and GPS, *Geophys. Res. Lett.*, *31*, L24605, doi:10.1029/2004GL021435.

Farrell, W. E. (1972), Deformation of the Earth by surface loads, *Rev. Geophys.*, *10*, 761–797.

Freeden, W., T. Gervens, and M. Schreiner (1998), *Constructive Approximation on the Sphere (With Applications to Geomathematics)*, Clarendon, Oxford, U. K.

Han, S.-C., C. K. Shum, C. Jekeli, and D. Alsdorf (2005), Improved estimation of terrestrial water storage changes from GRACE, *Geophys. Res. Lett.*, *32*, L07302, doi:10.1029/2005GL022382.

Han, S.-C., C. K. Shum, and C. Jekeli (2006), Precise estimation of in situ geopotential differences from GRACE low-low satellite-to-satellite tracking and accelerometer data, *J. Geophys. Res.*, doi:10.1029/2005JB003719, in press.

Jekeli, C. (1999), The determination of gravitational potential differences from satellite-to-satellite tracking, *Celestial Mech. Dyn. Astron.*, *75*, 85–100.

Kalnay, E., et al. (1996), The NCM/NCAR 40-year reanalysis project, *Bull. Am. Meteorol. Soc.*, *77*, 437–471.

Koch, K. R., and J. Kusche (2001), Regularization of geopotential determination from satellite data by variance components, *J. Geod.*, *76*(5), 259–268.

Milly, P. C. D., and A. B. Shmakin (2002), Global modeling of land water and energy balances, part I: The Land Dynamics (LaD) model, *J. Hydrometeorol.*, *3*, 283–299.

Reigber, C., R. Schmidt, F. Flechtner, R. König, U. Meyer, K.-H. Neumayer, P. Schwintzer, and S. Zhu (2005), An Earth gravity field model complete to degree and order 150 from GRACE: EIGEN-GRACE02S, *J. Geodyn.*, *39*, 1–10.

Rowlands, D., S. Luthcke, S. Klosko, F. Lemoine, D. Chinn, J. McCarthy, C. Cox, and O. Anderson (2005), Resolving mass flux at high spatial and temporal resolution using GRACE intersatellite measurements, *Geophys. Res. Lett.*, *32*, L04310, doi:10.1029/2004GL021908.

Schmidt, M., J. Kusche, J. van Loon, C. K. Shum, S.-C. Han, and O. Fabert (2005), Multi-resolution representation of regional gravity data, in *Gravity, Geoid and Space Missions*, *Int. Assoc. of Geod. Symp. Ser.*, vol. 129, edited by C. Jekeli, L. Bastos, and J. Fernandes, pp. 167–172, Springer, New York.

Swenson, S., and J. Wahr (2002), Methods for inferring regional surface-mass anomalies from satellite measurements of time variable gravity, *J. Geophys. Res.*, *107*(B9), 2193, doi:10.1029/2001JB000576.

Tapley, B. D., S. Bettadpur, M. Watkins, and C. Reigber (2004a), The Gravity Recovery and Climate Experiment: Mission overview and early results, *Geophys. Res. Lett.*, *31*, L06619, doi:10.1029/2003GL019285.

Tapley, B. D., S. Bettadpur, J. Ries, P. Thompson, and M. Watkins (2004b), GRACE measurements of mass variability in the Earth system, *Science*, *305*, 503–505.

S.-C. Han and C. K. Shum, Laboratory for Space Geodesy and Remote Sensing Research, Ohio State University, Columbus, OH 43210, USA. (han.104@osu.edu; ckshum@osu.edu)

J. Kusche, DEOS, Delft University of Technology, 2600 G3 Delft, Netherlands. (j.kusche@lr.tudelft.nl)

L. Sanchez and M. Schmidt, Deutsches Geodätisches Forschungsinstitut, Alfons-Goppel-Strasse 11, D-80539 Munich, Germany. (schmidt@dgfi.badw.de; sanchez@dgfi.badw.de)